Lasers in Manufacturing Conference 2021

High-speed synchrotron X-ray investigation of full penetration welding of aluminum sheets

Jonas Wagner[a,*], Christian Hagenlocher[a], Marc Hummel[b], Alexander Olowinsky[c], Rudolf Weber[a], Thomas Graf[a]

[a]*Institut für Strahlwerkzeuge IFSW, Universität Stuttgart, Pfaffenwaldring 43, 70569 Stuttgart, Germany*
[b]*Chair for Laser Technology LLT, RWTH Aachen University, , Steinbachstr. 15, 52074 Aachen, Germany*
[c]*Fraunhofer Institute for Laser Technology ILT, Steinbachstr. 15, 52074 Aachen, Germany*

Abstract

Full-penetration laser beam welding of aluminum alloys is widely applied in industrial welding processes of sheet metal components. It is characterized by a capillary, which fully penetrates two or more sheets in overlap configuration and is open at its top and bottom. Compared to partial penetration laser beam welding, full-penetration welding is associated with a stable capillary and therefore a more reliable process because the additional opening at the bottom side results in the avoidance of a collapsing capillary tip. The behavior of the capillary was analyzed by means of high-speed synchrotron X-ray imaging at the DESY for welding of aluminum sheets with thicknesses of 1 mm. The results prove the stabilization of the capillary if it opens at the bottom side of the sheet. Additionally, a stabilization of the melt-pool isotherm in front of the capillary is observed. Despite the reliable avoidance of capillary collapses, the formation of pores is still observed.

Keywords: laser beam welding; aluminum; full-penetration; X-ray imaging; synchrotron; pore formation

1. Introduction

During full-penetration laser beam welding a weld seem is formed whose depth corresponds to the thickness of the welded sheet metal. The application of this process enables a convenient verification whether the required penetration depth was reached by visual inspection of the bottom side of the sheet. Therefore, full-penetration welding is widely used in industrial applications. Research on full-penetration welding

* Corresponding author. Tel.: +49(0) 711 685-66849; fax: +49(0) 711 685-66842.
E-mail address: jonas.wagner@ifsw.uni-stuttgart.de.

involved high-speed video imaging of the top and bottom of the capillary, as shown by Fabbro et al., 2005, numerical analysis, as demonstrated by Vázquez et al., 2014 and the use of high-speed X-ray imaging, shown by Hagenlocher et al., 2020.

There are two modes of full-penetration welding which differ in stability and absorptance, as shown in Wagner et al., 2021. Fig. 1 shows these two modes of full-penetration. Both modes create a visible weld seam on the lower surface of the sheet. Mode A with a capillary whose depth s_c is less than the material's thickness s_s, as shown in Fig. 1a and mode B with a capillary whose depth equals the material's thickness and which is opened at its bottom, as shown in Fig. 1b. Compared to mode A this is associated with a more reliable process because the additional opening at the bottom side results in the avoidance of a collapsing capillary tip, as shown by Chang et al., 2015. In the present proceeding, the process stability during the two modes is compared.

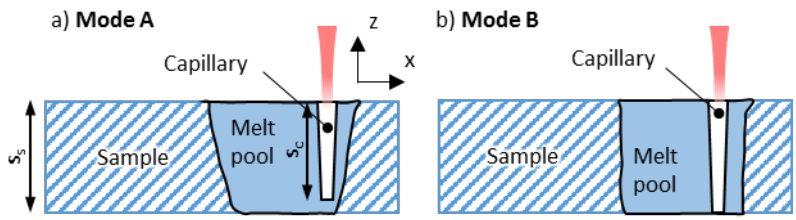

Fig. 1 Schematic diagram of the two modes of full-penetration welding. a) Mode A with a capillary which is closed at its bottom. b) Mode B with a capillary which is opened at its bottom.

A distinction by visual inspection between the two modes is only possible to a limited extend. Therefore, the stability of the capillary for each mode was analyzed by means of synchrotron X-ray radiation.

2. Setup

The stability of the capillary was analyzed by means of high-speed X-ray imaging at the DESY (Deutsches Elektronen-Synchrotron, Hamburg, Germany) for welding of Al99.5 (AA1050A) aluminum sheets with thicknesses of 1 mm. The set-up is described in detail in previous work by Wagner et al., 2021. Details about the DESY facility and the used beam line were described by Schell et al., 2013.

3. Results

For all trials the process parameters were chosen such that a visible weld seam on both sides of the sheet was present, i.e. the melt-pool isotherm reaches the lower surface of the sample. In order to archive welding in Mode A and Bode B the laser power was adapted correspondingly during the trials. The mode of full-penetration was distinguished by visual inspection of the measured penetration depth of the capillary. The remaining process parameters were kept constant with a feed rate v = 6 m/min and a spot diameter on the sample's surface d_f = 102 µm resulting in a laser power of P = 1.0 kW for welding in mode A and P = 1.2 kW for welding in mode B. The sheet was moved from right to left beneath the stationary focusing optics.

Fig. 2 shows single frames from the recorded high-speed X-ray videos taken at different times during welding , which are accessible for download in the supplementary material of previous work by Wagner et al., 2021. Fig. 2a to Fig. 2d show frames of the welding process in full-penetration mode A with P = 1.0 kW. Fig. 2e to Fig. 2h show frames of the welding process in full-penetration mode B with P = 1.2 kW.

The areas with a high grayscale value correspond to locations with an increased transmission of the X-ray beam. This occurs in areas with less material (in the direction of the X-rays) or with a reduced density, allowing

the identification of the capillary (indicated with an arrow in Fig. 2a and Fig. 2e). The transition from the solid to the liquid physical state causes interference effects of the transmitted, coherent X-ray beam on the scintillator, as described by van der Veen and Pfeiffer, 2004. This interference effect results in a decreased local grayscale value at the location of the transition from the solid to the liquid phase. From this local decrease, the local melt-pool isotherm can be identified (indicated with the arrows in Fig. 2b and Fig. 2f), as well as the boundaries of bubbles with gaseous content, which result in pores after solidification (indicated with the arrows in Fig. 2c and Fig. 2g).

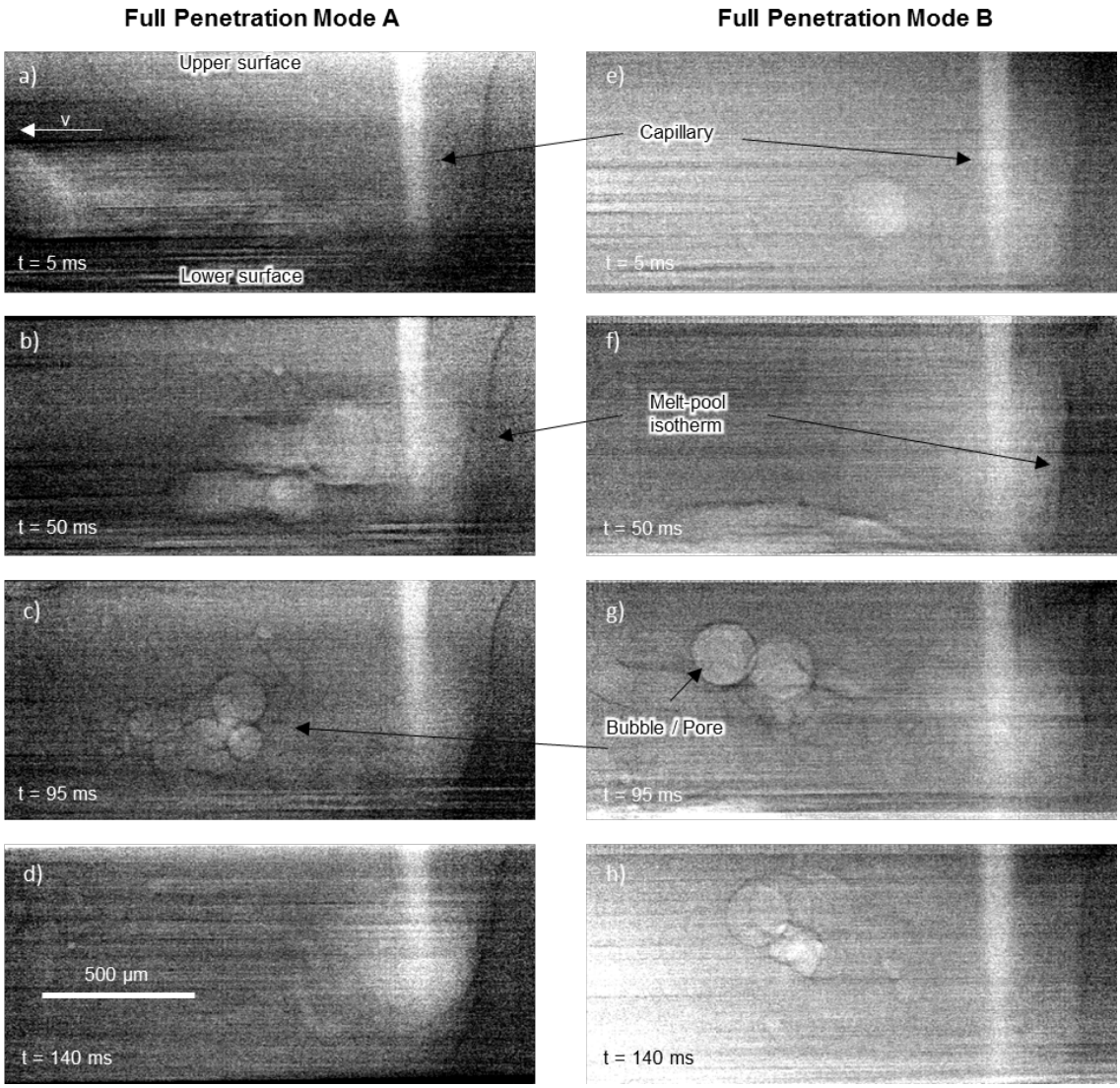

Fig. 2 Single frames at different times from high-speed X-ray videos of laser beam welding of AA1050A with d_f = 102 µm. Colum left, a) to d) full-penetration Mode A with P = 1.0 kW, column right, e) to h) full-penetration Mode B with P = 1.2 kW. (Whole image sequence given with video S1 in supplementary of Wagner et al., 2021)

The capillary, which is closed at the bottom in Fig. 2a to Fig. 2d, proves that the lower laser power leads to welding in full-penetration mode A. In comparison the higher laser power of 1.2 kW leads to a capillary which is open at its bottom, as shown in Fig. 2e to Fig. 2h. In both cases full-penetration welding is ensured by the melt-pool isotherm which expands from the upper surface to the lower surface of the sheet. The melt-pool isotherm in front of the capillary shows a S-shaped course in case of mode A (see Fig. 2a to Fig. 2d), while it is a straight vertical line in case of mode B.

The closed capillary in case of mode A showed pronounced dynamic changes of its shape. In particular, its depth fluctuated strongly. These changes in depth coincide with changes of the absorptance of the laser beam in the capillary, as shown by Gouffé, 1945 with minor corrections from Hügel and Graf, 2014. As a consequence, the energy input changes dynamically during the welding process, which is represented by the fluctuation of the shape of the melting isotherm in front of the capillary.

In case of welding with full-penetration in mode B the shape of the capillary stays constant without significant fluctuations. As a consequence, the absorptance and the energy input is constant, which is confirmed by the stable melting process which is indicated by the constant shape and position of the melt-pool isotherm in front of the capillary.

4. Summary

The stability of the capillary and the melt-pool isotherm in front of the capillary during the two modes of full-penetration welding were investigated by means of high-speed synchrotron X-ray imaging. The results prove that two modes of full-penetration welding occur. Mode A with a capillary, which is closed at its bottom and, when the laser power is increased, mode B with a capillary which is opened at its bottom. As reported by Chang et al., 2015 mode B results in a stable penetration depth of the capillary. Furthermore, it could be shown that this also leads to a constant melting process. Despite the reliable avoidance of capillary collapses, the formation of pores is still observed in mode B. Therefore, this must be related to a different mechanism e.g. evaporation of lubricants as observed by Hagenlocher et al., 2020.

Acknowledgements

This work was funded by the Deutsche Forschungsgemeinschaft (DFG, German Research Foundation)—266218804.

This research was supported by TRUMPF GmbH & Co. KG. The presented investigations were carried out in cooperation with DESY in Hamburg and with RWTH Aachen University within the framework of the Collaborative Research Centre SFB1120-236616214 “Bauteilpräzision durch Beherrschung von Schmelze und Erstarrung in Produktionsprozessen” and funded by the Deutsche Forschungsgemeinschaft e.V. (DFG, German Research Foundation). We acknowledge DESY (Hamburg, Germany), a member of the Helmholtz Association HGF, for the provision of experimental facilities. Parts of this research were carried out at PETRA III and we would like to thank F. Beckmann and J. Moosmann for assistance in using P07 EH4. Beamtime was allocated for proposal I-20191140. The sponsorship and support is gratefully acknowledged.

References

Chang B., Allen C., Blackburn J., Hilton P., Du D., 2015. Fluid Flow Characteristics and Porosity Behavior in Full Penetration Laser Welding of a Titanium Alloy. Metall and Materi Trans B 46, pp 906–918. doi: 10.1007/s11663-014-0242-5

Fabbro R., Slimani S., Coste F., Briand F., 2005. Study of keyhole behaviour for full penetration Nd–Yag CW laser welding. J. Phys. D: Appl. Phys. 38, pp 1881–1887. doi: 10.1088/0022-3727/38/12/005

Gouffé A., 1945. Corrections d'ouverture des corps-noirs artificiels compte tenu des diffusions multiples internes. Rev. opt. 24, pp 1–7

Hagenlocher C., Lind J., Weber R., Graf T., 2020. High-Speed X-Ray Investigation of Pore Formation during Full Penetration Laser Beam Welding of AA6016 Aluminum Sheets Contaminated with Lubricants. Applied Sciences 10, p 2077. doi: 10.3390/app10062077

Hügel H., Graf T. (2014). Laser in der Fertigung: Grundlagen der Strahlquellen, Systeme, Fertigungsverfahren, 3rd edn. Lehrbuch. Springer Vieweg, Wiesbaden

Schell N., King A., Beckmann F., Fischer T., Müller M., Schreyer A., 2013. The High Energy Materials Science Beamline (HEMS) at PETRA III. MSF 772, pp 57–61. doi: 10.4028/www.scientific.net/MSF.772.57

van der Veen F., Pfeiffer F., 2004. Coherent x-ray scattering. J Phys Condens Matter 16, pp 5003–5030. doi: 10.1088/0953-8984/16/28/020

Vázquez R. G., Koch H. M., Otto A., 2014. Multi-physical Simulation of Laser Welding. Physics Procedia 56, pp 1334–1342. doi: 10.1016/j.phpro.2014.08.059

Wagner J., Hagenlocher C., Hummel M., Olowinsky A., Weber R., Graf T., 2021. Synchrotron X-Ray Analysis of the Influence of the Magnesium Content on the Absorptance during Full-Penetration Laser Welding of Aluminum. Metals 11, p 797. doi: 10.3390/met11050797